STRUCTURAL BIOLOGY COMMUNICATIONS

Volume 77 (2021)

Supporting information for article:

Crystal structure of acetylxylan esterase from *Caldanaerobacter subterraneus* subsp. *tengcongensis*

Kohei Sasamoto, Tomoki Himiyama, Kunihiko Moriyoshi, Takashi Ohmoto, Koichi Uegaki, Yoshiaki Nishiya and Tsutomu Nakamura

Table S1. In-fusion cloning primers.

Name	Sequence (5′ to 3′)
pET32b linear forward primer	GCCATGGCGATATCGGATCCGAATTCGAGCTCCGTC
pET32b linear reverse primer	AAACAGAACTTCCAGGCTGTCCATGTGCTGGCG
TTE0866 forward primer	CTGGAAGTTCTGTTTCAAGGTCCGTACAAATACATCACTGAAGAT
TTE0866 reverse primer	CGATATCGCCATGGCTTAATCCCTCTTTTCTAAAAG

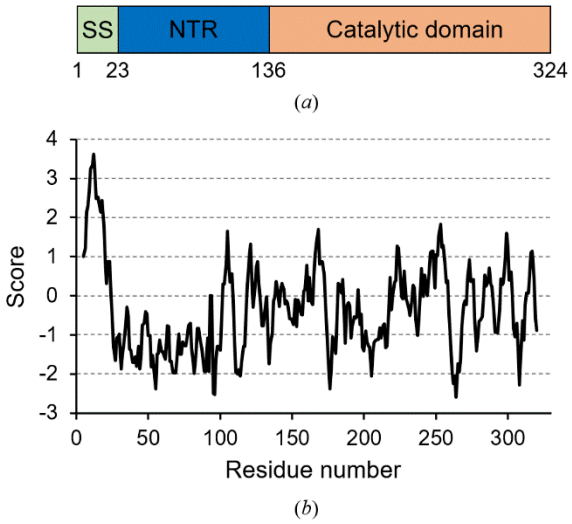

Figure S1. Schematic structure of domains of TTE0866 (*a*) and hydropathy plot (*b*). SS: signal sequence; NTR: N-terminal region.

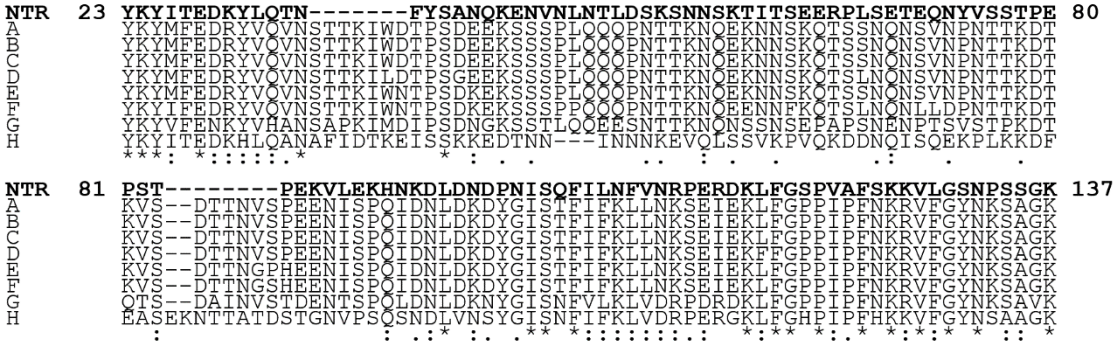

Figure S2. Sequence alignment of NTR and its homologous proteins. Source of NTR is *Thermoanaerobacter tengcongensis* (accession number: AAM24122). Sources of A–H are (A) *Thermoanaerobacter* sp. (HHY79381.1), (B) *Thermoanaerobacter thermohydrosulfiricus* (EMT38705.1), (C) *Thermoanaerobacter ethanolicus* (EGD50256.1), (D) *Thermoanaerobacter* sp. (MBE3591604.1), (E) *Thermoanaerobacter uzonensis* (SHF11829.1), (F) *Thermoanaerobacter* sp. YS13 (KHO62125.1), (G) *Thermoanaerobacter kivui* (AIS52065.1), and (H) *Clostridium* (HHW56946.1).

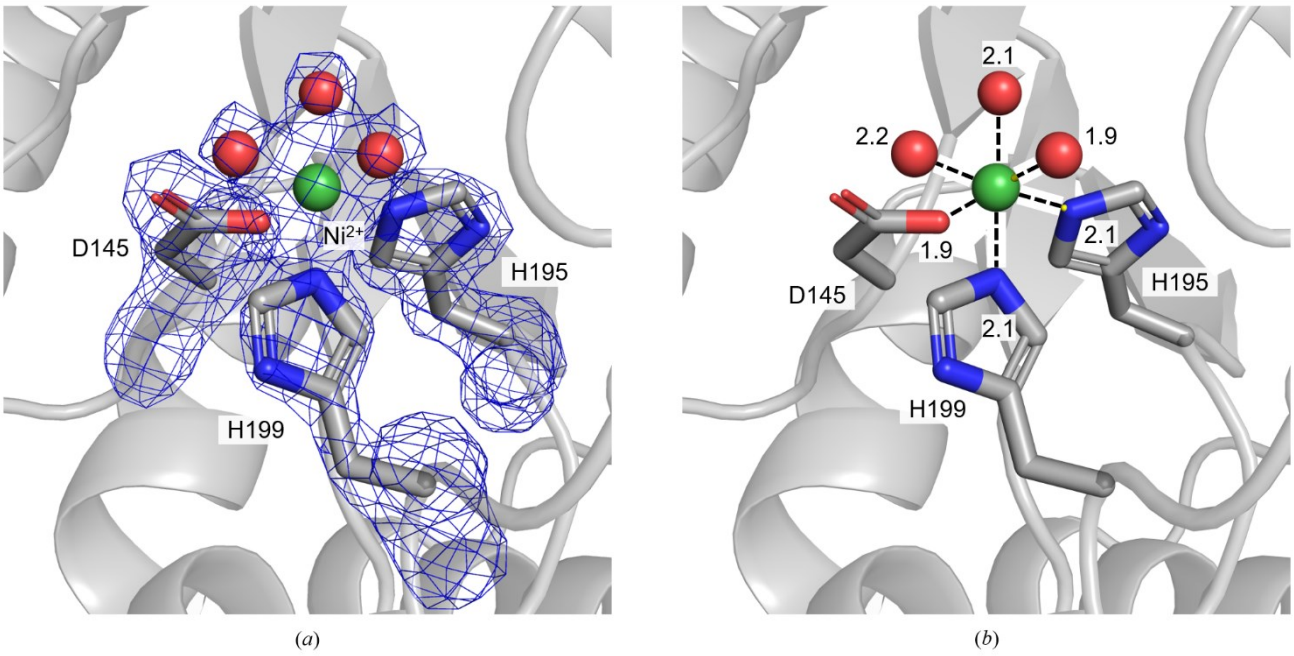

Figure S3. (*a*) F_o-F_c omit map of the metal-binding triad and metal ion and (*b*) the distance between the ligands. The metal-binding triad of Asp145, His195, and His199 (MT1 and MT2) are shown as gray sticks. Ni^{2+} is shown as green sphere. Three water molecules bound to the central metal are shown as red spheres. The F_o-F_c omit map is contoured at 4.5 σ level in blue mesh. The interaction between ligands is shown as black dashed lines with distances in Å.

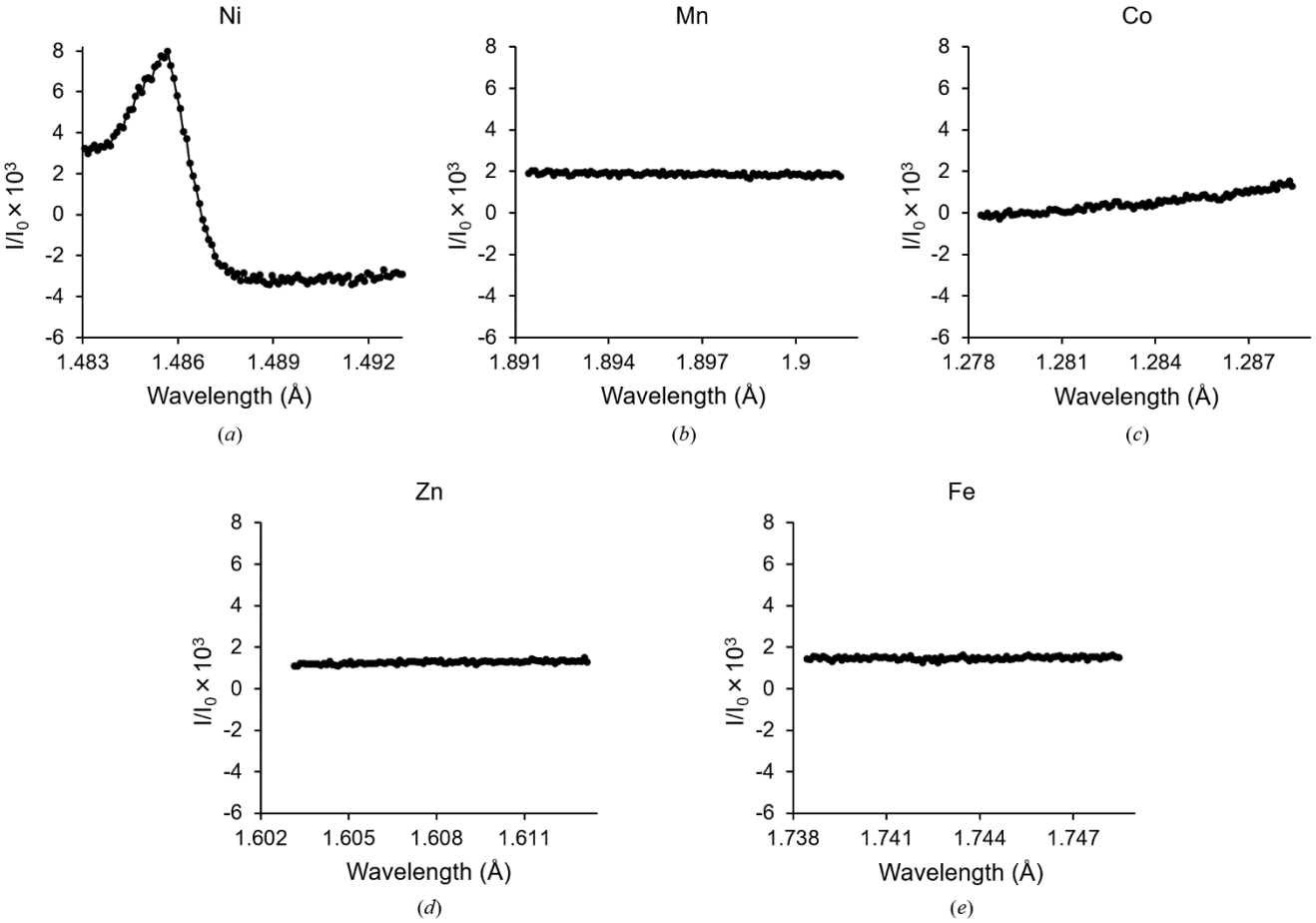

Figure S4. XAFS spectra of a TTE0866 crystal around the (*a*) Ni Kα, (*b*) Mn Kα, (*c*) Co Kα, (*d*) Zn Kα and (*e*) Fe Kα absorption edges.

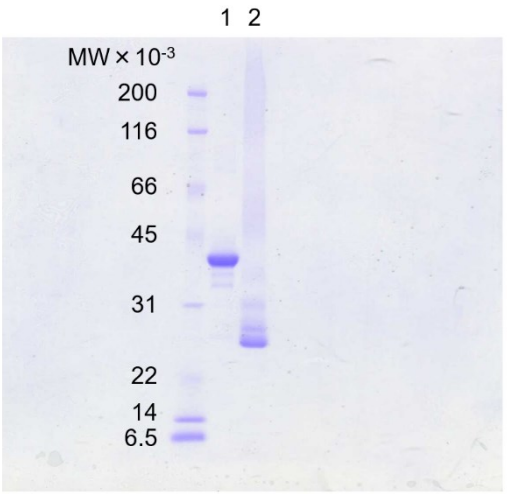

Figure S5. SDS–PAGE of TTE0866 (lane 1) and TTE0866 crystals dissolved in a 20 mM Tris-HCl (pH 8.0) buffer (lane 2).

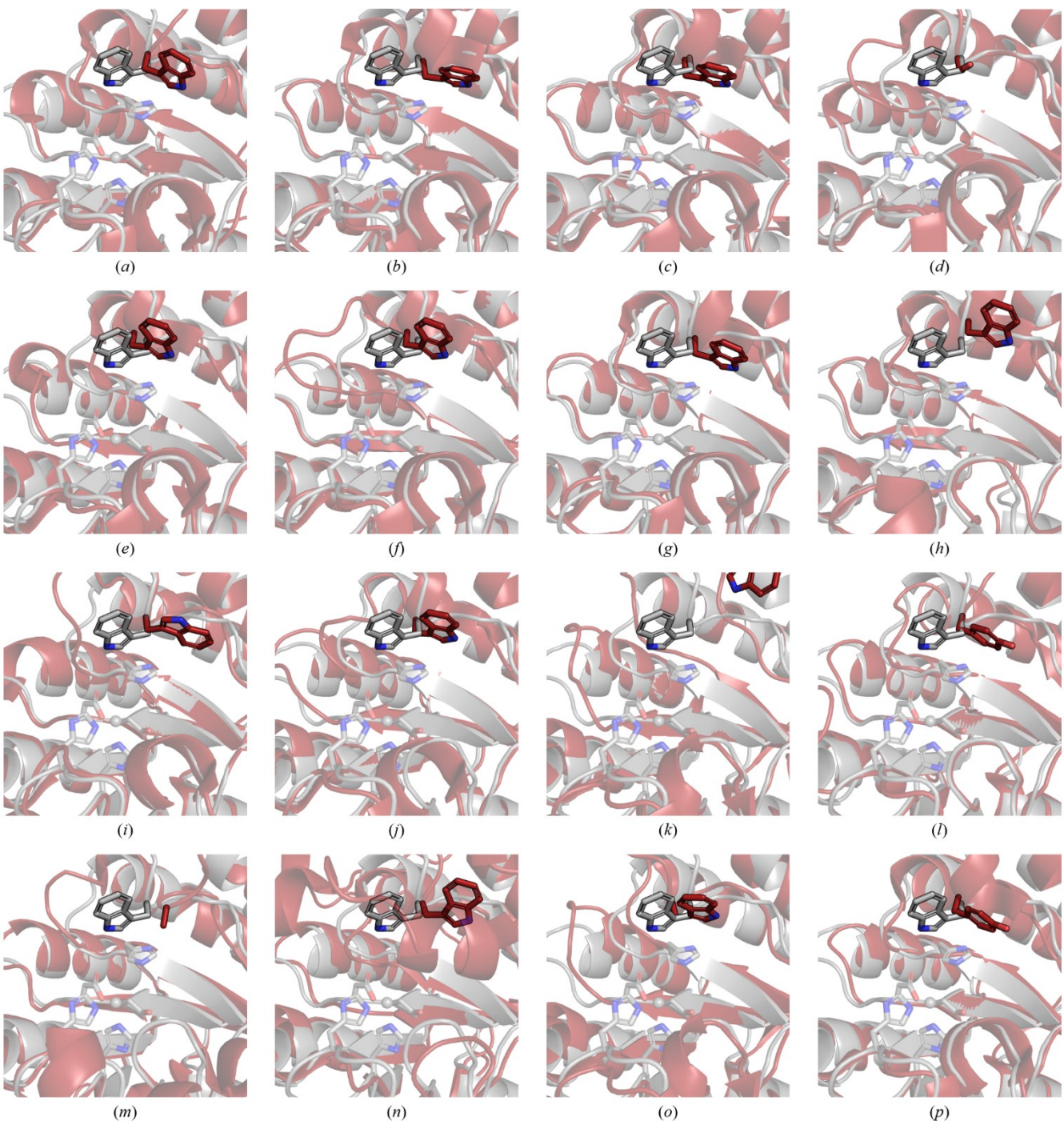

Figure S6. Orientation of aromatic amino acid residues in MT4 of CE4 enzymes. The W264 residue of TTE0866 and its corresponding residues in other CE4 enzymes are represented as gray and red stick models, respectively. Each figure letter corresponds to Table 1. (*a*) The W402

residue of BsPdaC (*Bacillus subtilis* subsp. *subtilis*), (*b*) the W171 residue of ArCE4 (*Arthrobacter* sp.), (*c*) the W131 residue of SlAXE (*Streptomyces lividans*), (*d*) the S708 residue of Xyl-CE4 (uncultured bacterium), (*e*) the W213 residue of BA3943 (*B*. *anthracis*), (*f*) the W200 residue of BcPdgA (BC1960; *B*. *cereus*), (*g*) the W392 residue of SpPgdA (*Streptococcus pneumoniae*), (*h*) the W198 residue of BC1974 (*B*. *cereus*), (*i*) the W604 residue of CtAXE (*Acetivibrio thermocellus*), (*j*) the W185 residue of BA0150 (*B*. *anthracis*), (*k*) the W173 residue of BaCE4 (BA0424) (*B*. *anthracis*), (*l*) the Y173 residue of ClCDA (*Colletotrichum lindemuthianum*), (*m*) the A246 residue of SmPgdA (*Streptococcus mutans*), (*n*) the W308 residue of Bd3279 (*Bdellovibrio bacteriovorus*), (*o*) the W194 residue of BsPgaA (*B*. *subtilis*), and (*p*) the Y166 residue of AnCDA (*Aspergillus nidulans*).